



TANG FRAGMENT OF A KNIFE HR-6246 - TIN BRONZE - LATE BRONZE AGE - SWITZERLAND

Artefact name Tang fragment of a knife HR-6246

Authors Marianne. Senn (Empa, Dübendorf, Zurich, Switzerland) & Christian. Degrigny (HE-Arc CR, Neuchâtel, Neuchâtel, Switzerland) & Naima. Gutknecht

(HE-Arc CR, Neuchâtel, Neuchâtel, Switzerland) & Rémy. Léopold (HE-Arc CR, Neuchâtel, Neuchâtel, Switzerland)

Url /artefacts/1230/

▼ The object

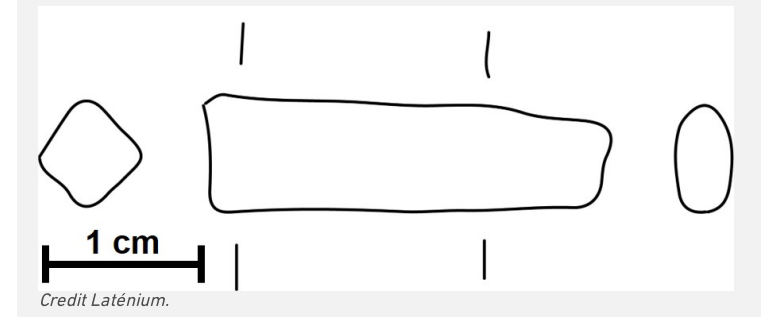


Fig. 1: Tang fragment of a knife (after Rychner-Faraggi 1983, plate 35.35),



Fig. 2: Shiny yellow and green-blue corrosion products on the surface of the tang fragment of a knife,

▼ Description and visual observation

Description of the artefact Tang fragment of a knife with shiny yellow and green-blue corrosion products (Figs. 1 & 2). Dimensions: L = 2.7cm; $\emptyset = around 5mm$;

WT = 5.8q.

Type of artefact Household implement

Origin Hauterive - Champréveyres, Neuchâtel, Neuchâtel, Switzerland

Recovering date Excavation 1983-1985, object from layer 1 (layer with material from Bronze Age till 20th cent.)

Chronology category Late Bronze Age

chronology tpq 1050

chronology taq B.C. 🗸 800

Hallstatt A/B Chronology comment

Burial conditions / environment Lake



Artefact location Laténium, Neuchâtel, Neuchâtel

Owner Laténium, Neuchâtel, Neuchâtel

Inv. number Hr 6246

Recorded conservation data N/A

Complementary information

The object was sampled in 1987 for analysis. Documentation of the strata in binocular mode on the remaining fragment of the object was performed in 2022.

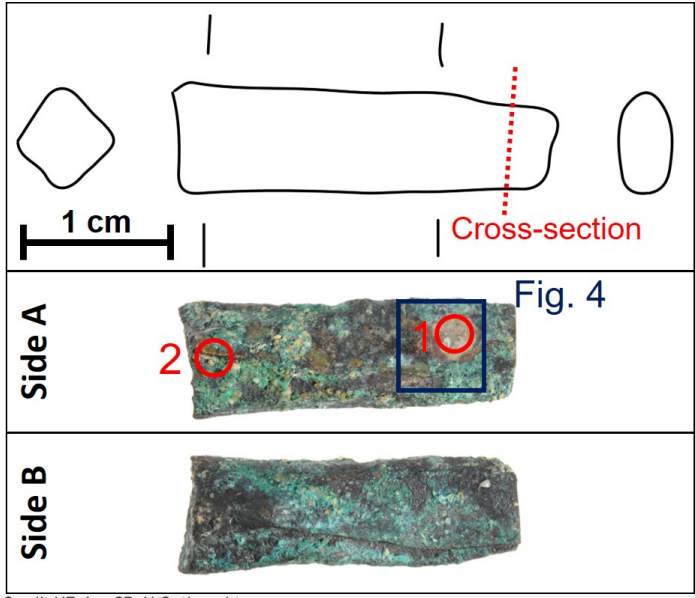


Fig. 3: Location of the cross-section before sampling and both sides of the fragment not sampled with location of the detail of Fig. 4 (blue square) and XRF analysis areas (red circles).

Credit HE-Arc CR, N.Gutknecht.

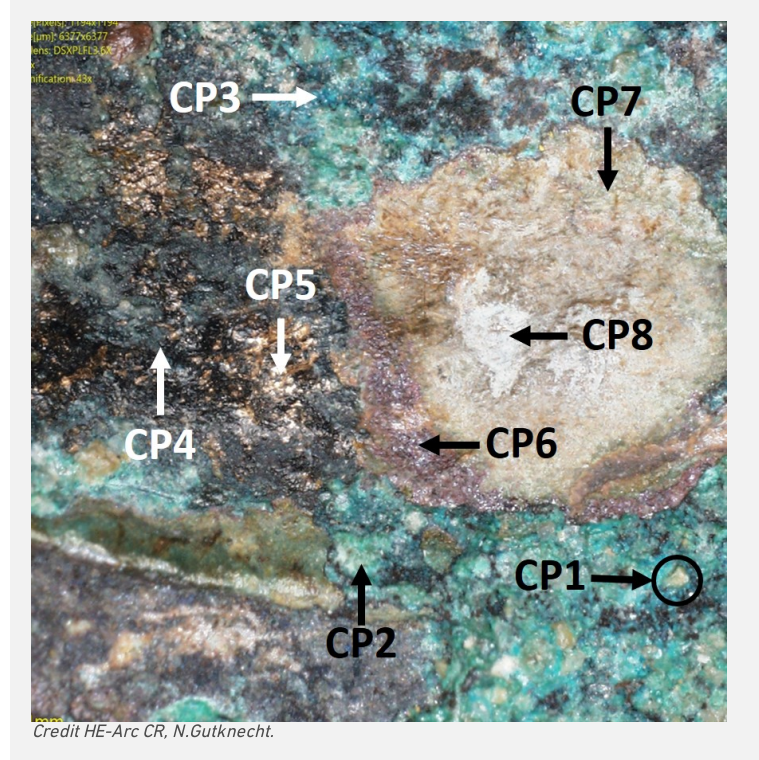


Fig. 4: Corrosion structure (detail) from Fig. 3 showing some of the documented strata,

Binocular observation and representation of the corrosion structure

The schematic representation below gives an overview of the corrosion structure encountered on the tang from a first visual macroscopic observation.

Strata	Type of stratum	Principal characteristics

CP1	Corrosion product	Nodule, light brown, thin, scattered, compact, severable, very soft
CP2	Corrosion product	Dark green, submetallic, thin, scattered, compact, tough, soft
CP3	Corrosion product	Blue, submetallic, thin, scattered, compact, tough, soft
CP4	Corrosion product	Black, resinous, thin, discontinuous, compact, malleable, very soft
CP5	Corrosion product	Yellow, metallic, medium (thickness), discontinuous, compact, brittle, hard
CP6	Corrosion product	Red, adamantine, thin, continuous, non-compact, friable, soft
CP7	Corrosion product	Light brown, matte, thin, continuous, compact, friable, soft
CP8	Corrosion product	Light yellow, matte, thin, continuous, non-compact, powdery, very soft
M1	Metal	Yellow, thick, metallic, soft

Table 1: Description of the principal characteristics of the strata as observed under binocular and described according to Bertholon's method.

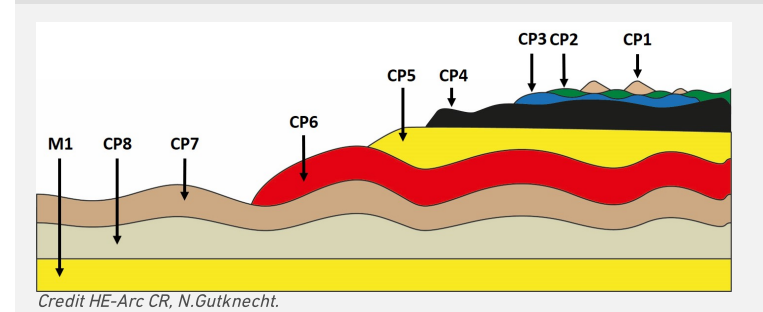


Fig. 5: Stratigraphic representation of the corrosion structure of the tang by macroscopic and binocular observation with reference to Fig. 4,

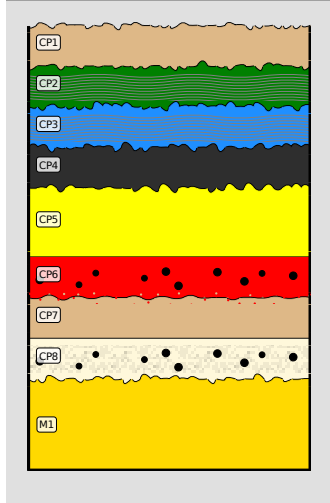


Fig. 6: Stratigraphic representation of the corrosion structure of the tang observed macroscopically under binocular microscope using the MiCorr application with reference to the whole Fig. 5. The characteristics of the strata, such as discontinuity, are accessible by clicking on the drawing that redirects you to the search tool by stratigraphy representation, Credit HE-Arc CR, N.Gutknecht,

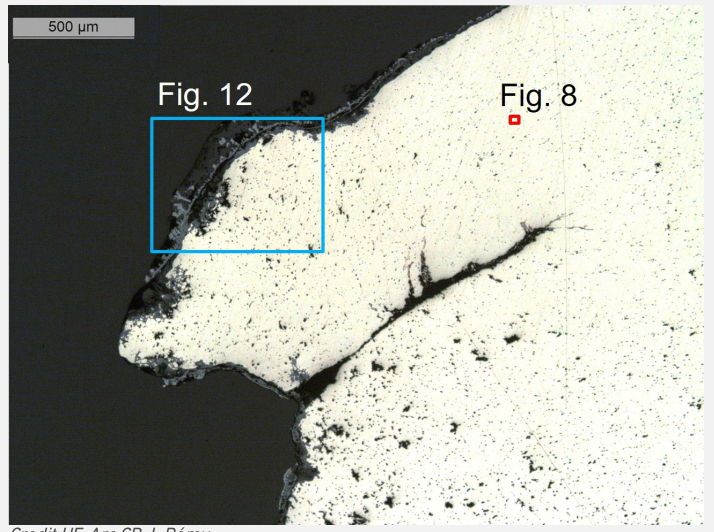


Fig. 7: Micrograph from an area of the cross-section of the sample taken from the tang fragment with location of Fig. 8 (red square) and Fig. 12 (blue square), unetched, bright field,

Credit HE-Arc CR, L.Rémy.

Description of sample

The cross-section corresponds to a lateral cut (Fig. 3). The surface is covered with a thick corrosion layer but part of it has gone (Fig.

7).

Alloy Tin Bronze

Technology Cold worked with partial annealing

Lab number of sample MAH 87-197

Sample location Musées d'art et d'histoire, Genève, Geneva

Responsible institution Musées d'art et d'histoire, Genève, Geneva

Date and aim of sampling 1987, metallography and corrosion characterisation

Complementary information

This sample is mentioned in Schweizer, 1994.

Analyses performed:

Non-invasive approach

XRF with handheld portable X-ray fluorescence spectrometer (NITON XL5). General Metal mode, acquisition time 60s (filters: Li20/Lo20/M20).

Invasive approach (on the sample)

Metallography (etched with ferric chloride reagent), Vickers hardness testing, ICP-OES (conditions provided in the About tab of the MiCorr application), SEM/EDS (20keV, Microcity), XRD

▼ Non invasive analysis

XRF analyses of the tang fragment were carried out on two representative areas (Fig. 3). Point 1 was done in a lacuna of the green-blue corrosion layer, while point 2 was performed on a black corrosion layer (CP4) where all strata (soil, corrosion products, and metal) are analyzed at the same time.

The metal is presumably a tin bronze alloy. The other elements detected are: S, Si, Pb, Sb, Fe, As, Ni, Ag, Zn, Co.

Both results are similar.

Elements (mass %)			:	Sn .	:	S		Si	F	b	:	Sb		Fe	,	As		Ni	,	Ag	2	Zn	C	Co	
	%	+/- 2σ	%	+/- 2σ	%	+/- 2σ	%	+/- 2σ	%	+/- 2σ	%	+/- 2σ	%	+/- 2σ	%	+/- 2σ	%	+/- 2σ	%	+/- 2σ	%	+/- 2σ	%	+/- 2σ	Total
1	83.0	0.1	10.0	0.05	2.5	0.03	1.5	0.05	0.5	0.02	0.5	0.02	0.4	0.02	0.4	0.03	0.3	0.01	0.2	0.01	0.1	0.02	<0.1	0.01	99.4
2	81.0	0.2	9.0	0.06	2.0	0.04	0.7	0.09	0.7	0.02	0.7	0.02	0.5	0.02	1.0	0.03	0.3	0.02	0.3	0.01	0.1	0.03	<0.1	0.01	99.3

Table 2: Chemical composition of the surface of the tang at two representative areas shown in Fig. 3. Method of analysis: XRF, UR-Arc CR.

The remaining metal is a tin bronze (Table 3) with high porosity (Figs. 7-9) and large cracks both on the left and right edges of the sample (Fig. 9). The metal contains small, elongated copper sulphide (Table 4) and Pb inclusions. The etched metal shows three zones with a core where elongated grains and slip lines are visible indicating cold working without annealing (Figs. 9-10), while annealing appears on both external sides (Fig. 9-11). The average hardness of the metal is HV1 145, but significant variations are observed, depending on where the measurements are taken.

	Cu		Sb		Pb		Ag	Со	Fe	Zn
mass%	89.85	8.02	0.60	0.55	0.34	0.34	0.18	0.10	0.02	0.01

Table 3: Chemical composition of the metal. Method of analysis: ICP-0ES, Laboratory of Analytical Chemistry, Empa.

Elements			Cu	
mass%	0.9	20	77	98

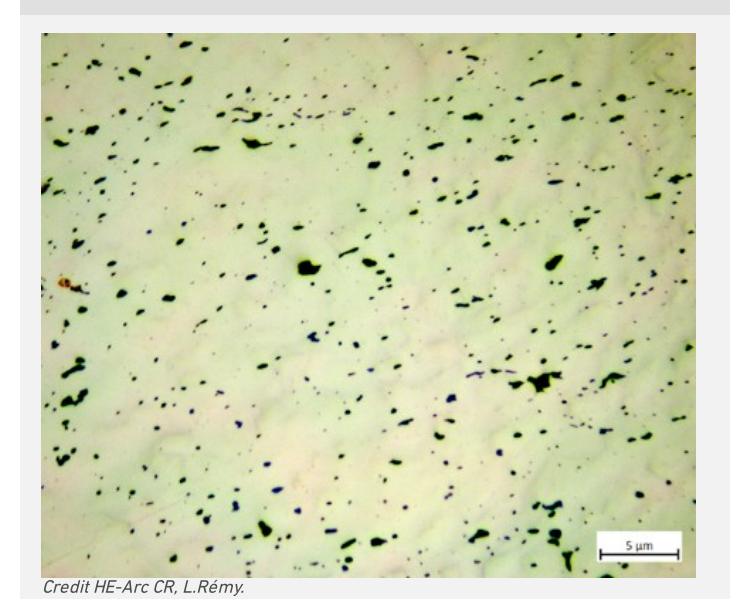


Fig. 8: Detail of the metal from Fig. 7, unetched, bright field,

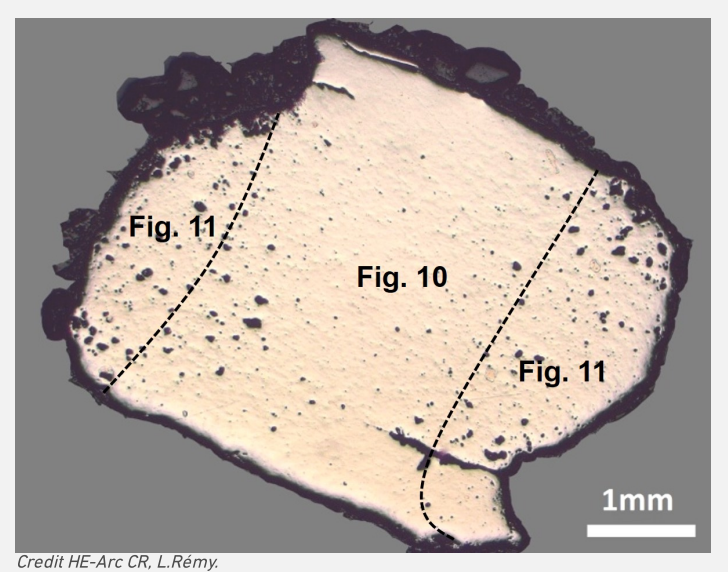


Fig. 9: Micrograph of the cross section of the tang of a knife with three distinct zones: metal core with elongated grains and slip lines (Fig. 10) and external sides with polygonal grains and twin lines (Fig. 11), unetched, bright field,

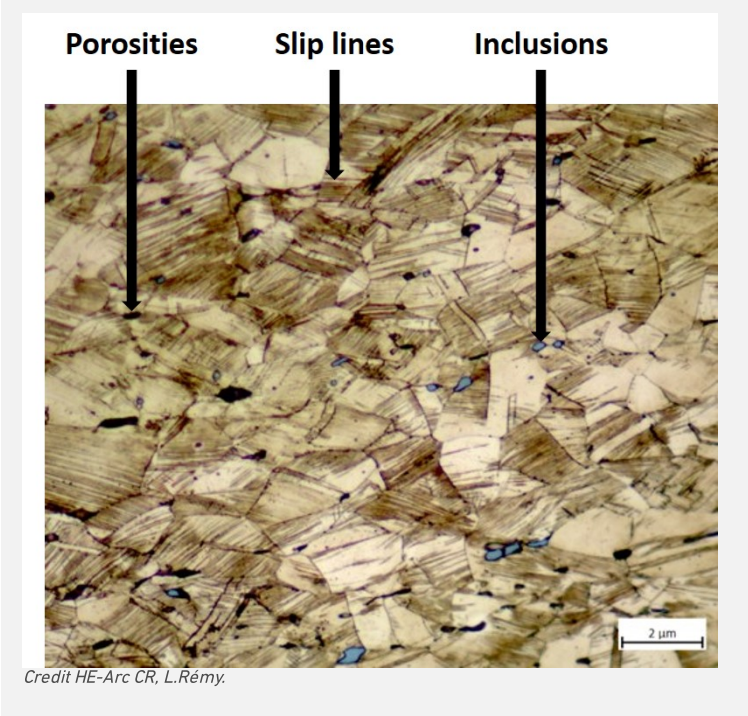
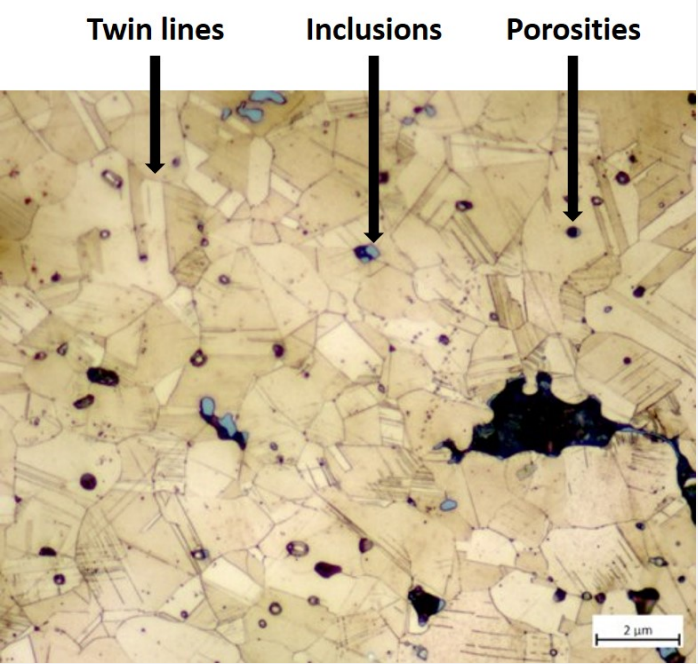


Fig. 10: Micrograph of the metal sample from Fig. 9 (detail), etched, bright field. Elongated grains with slip lines are observed, as well as grey copper sulphide inclusions and dark porosities,

Fig. 11: Micrograph of the metal sample from Fig. 9 (detail), etched, bright field. Twin lines, grey copper sulphide inclusions and dark porosity are observed,



Credit HE-Arc CR, L.Rémy.

Microstructure Mixture of elongated grains with slip lines and polygonal grains with twin lines

First metal element Cu

Other metal elements Co, Ni, As, Ag, Sn, Sb, Pb

Complementary information

Schweizer (1994) indicates that the copper-tin alloys similar to the one of the tang have minor constituents that were certainly not added intentionally. Furthermore, he mentions that there is no systematic composition difference between bronzes with a lake patina and those with a land patina.

The corrosion layer has a thickness between 130µm and 70µm (Fig. 12). The observation of the sample in cross-section (Figs. 12-13) shows the presence of a succession of layers: S1 sediment, at the very top surface; CP1 thick continuous layer, dark grey in bright field, dark turquoise in dark field; CP2 thin continuous layer which might expand through the whole CP1, extra light grey in bright field, black in dark field; CP3 thin continuous layer, extra light grey in bright field, light brown in dark field; CP4 medium continuous layer, light grey in bright field, dark orange in dark field; CP6 thin discontinuous layer, black in bright field, light brown in dark field; CM1 medium discontinuous layer;

The elemental chemical distribution (Fig. 15) of the SEM image (Fig. 14) of the visually identified strata by cross-sectional observation shows that:

S1 has Ca, Al, Si and O elements;

CP1 stratum contains Cu, O and S; CP2 stratum contains Cu, S and Fe;

CP3 stratum contains Sn, Fe and S;

CP4 stratum contains Sn and 0;

CP5 stratum contains Cu, O and S;

CP6 stratum contains Sn and O, similar to CP4;

XRD analyses indicated the presence of posnjakite/Cu4SO4(OH)6H2O, chalcocite/CuS and djurleïte/Cu1.93S (Schweizer 1994).

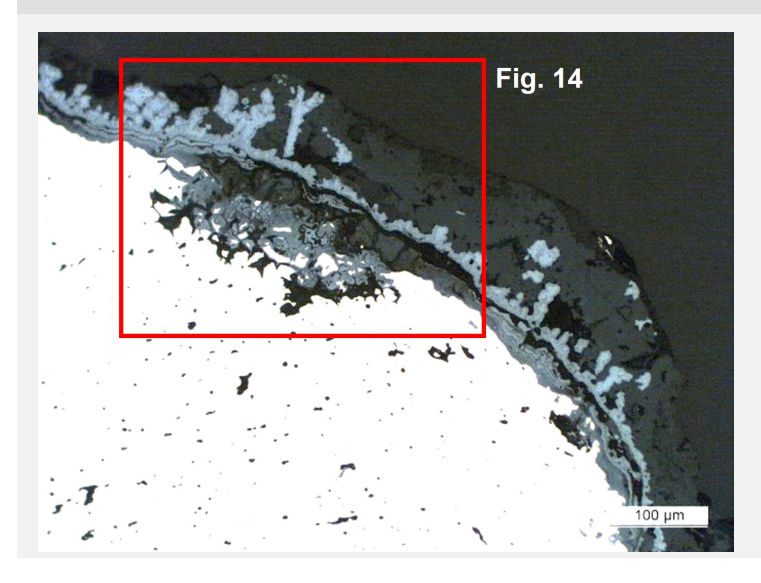


Fig. 12: Micrograph of the metal sample from Fig. 7 (detail, rotated of 90°), unetched, bright field.

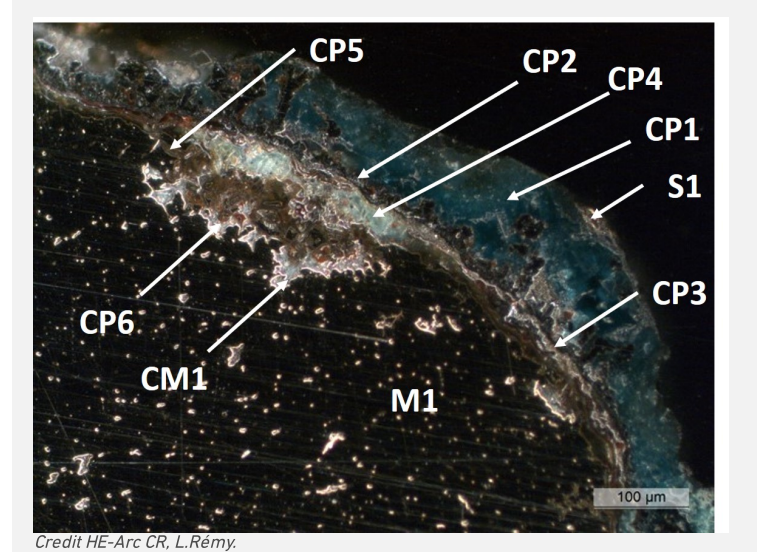
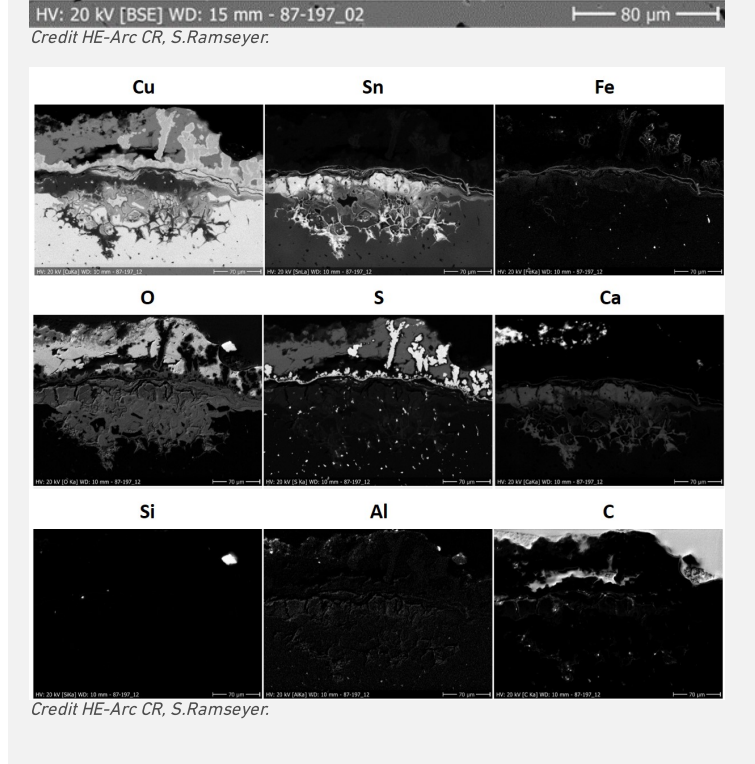


Fig. 13: Micrograph similar to Fig. 12, unetched, dark field and corresponding to the stratigraphy of Fig. 16,

Fig. 14: SEM image, BSE-mode (detail of Fig. 12),



Corrosion form

Corrosion type

Fig. 15: Elemental chemical distribution of Fig. 14 (reversed). Method of examination: SEM/EDS, Microcity,

Uniform - transgranular

Type I (Robbiola)

None.

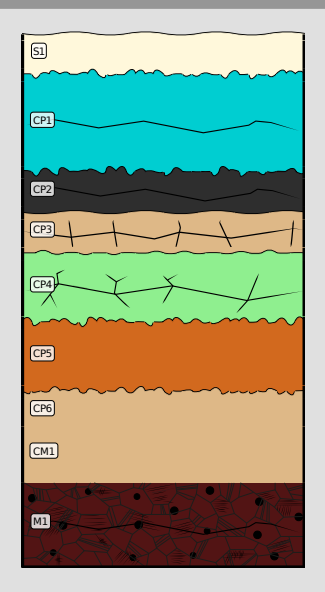


Fig. 16: Stratigraphic representation of the sample taken from the tang fragment in cross-section (dark field) using the MiCorr application. The characteristics of the strata are only accessible by clicking on the drawing that redirects you to the search tool by stratigraphy representation. This representation can be compared to Fig. 13, Credit HEARC CR, L.Rémy.

♥ Synthesis of the binocular / cross-section examination of the corrosion structure

The following correspondence can be found: CP1 in binocular mode as sediment (S1) in cross-section mode. CP2 and CP3 in binocular mode are differentiated by their color. They match CP1 in cross-section mode. CP4 in binocular mode matches CP2 in cross-section mode. CP5 in binocular mode seems to match CP3 in cross-section mode. CP6 and CP7 in binocular mode matches CP4 in cross-section mode. CP8 in binocular mode matches CP5, CP6 and CM1 in cross-section mode.

On cross-section, it was possible to describe and analyze the microstructure of the metal.

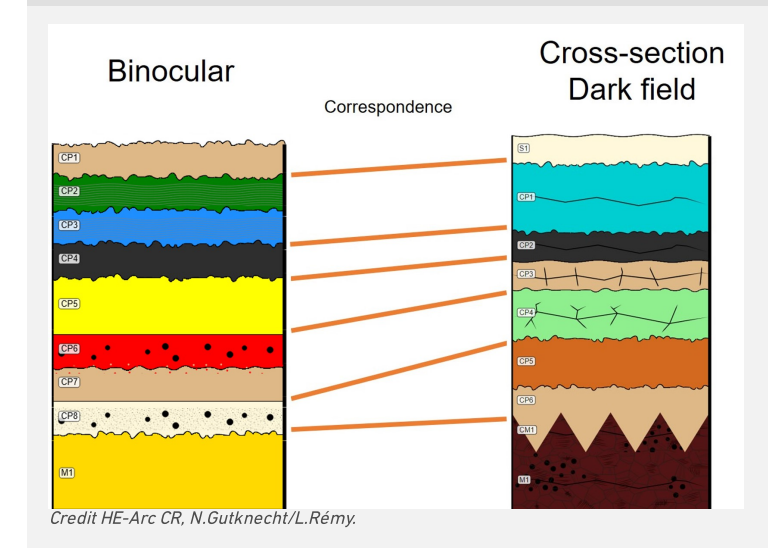


Fig. 17: Stratigraphic representation side by side of binocular view and cross-section (dark field)

▼ Conclusion

The tang fragment is made from a tin bronze and has been cold worked with partial annealing since slip lines are still visible. Past XRD analyses indicate the presence of chalcopyrite in the corrosion layer, typical of lake context (Schweizer 1994), which we seem to have found locally in the corrosion structure. This object was certainly abandoned rather quickly in an anaerobic, humid and S and Fe-rich environment, favouring then the formation of chalcopyrite, before being exposed in an aerated environment in which the corrosion structure was formed. The limit of the original surface most probably lies between the Sn-rich inner layer and the Fe/Cu and S-rich outer layers. The corrosion is a type 1 according Robbiola et al. 1998.

This object was first sampled in 1987. Thanks to an extensive documentation on the cross-section and comparison with similar objects (see references), Schweizer defines a "land patina" typology on this object.

▼ References

References on object and sample

Object files in MiCorr

- MiCorr_Pin or needle fragment HR-3031
 MiCorr_Tang fragment of a knife HR-6567
- 3. MiCorr_Pin HR-17773
- 4. MiCorr_Pin HR-3071

- MiCorr_Pin HR-18603
 MiCorr_Pin HR-3389
 MiCorr_Pin HR-18152

References object

8. Rychner-Faraggi A-M. (1993) Hauterive – Champréveyres 9. Métal et parure au Bronze final. Archéologie neuchâteloise, 17 (Neuchâtel).

References sample

- 9. Rapport d'examen, Laboratoire Musées d'art et d'histoire, Geneva GE (1987), 87-194 à 197.
- 10. Schwartz, G.M. (1934) Paragenesis of oxidised ores of copper, Economic Geology, 29, 55-75.
- 11. Schweizer, F. (1994) Bronze objects from Lake sites: from patina to bibliography. In: Ancient and historic metals, conservation and scientific research (eds. Scott, D.A., Podany, J. and Considine B.B.), The Getty Conservation Institute, 33-50.

References on analytic methods and interpretation

12. Robbiola, L., Blengino, J-M., Fiaud, C. (1998) Morphology and mechanisms of formation of natural patinas on archaeological Cu-Sn alloys, Corrosion Science, 40, 12, 2083-2111.